

Analysis of sediment transport from recorded signals of sediments in a gravel-bed river: role of sediment availability

Eric Travaglini¹, Eric Bardou¹, Christophe Ancey², Patricio Bohorquez³

¹ CREALP – Centre de Recherche en Environnement Alpin – Rue de l'industrie 45 – 1951 Sion – Switzerland

² School of Architecture, Civil and Environmental Engineering, Ecole Polytechnique Fédérale de Lausanne, 1015 Lausanne, Switzerland

³ Área de Mecánica de Fluidos, Departamento de Ingeniería Mecánica y Minera, Universidad de Jaén, Campus de las Lagunillas, 23071 Jaén, Spain

Abstract: Geophones were used as a proxy for determining the behavior of sediment transport in boulder mountain river. Field observations aggregated by a statistical analysis (PCA) allowed to identifying periods in which the behaviour between the water discharge (Q_w), the sediment flux (Q_s) and the meteorologic conditions was correlated. Within each period a relationship between Q_s and Q_w could be found and summarized by two parameters: the critical drag discharge for motion initiation (Q_d) and the mean transport rate (T_{mean}). The coefficients of determination were close to 0.8, which showed the consistency of the linear relationship.

The variability in the relationship $Q_s \sim Q_w$ could be related to the availability to motion of sediments. In contrast with laboratory experiments, in which sediment storage is indefinitely large, natural systems can suffer from sediment shortage under certain conditions. This may explain why bedload transport equations determined from laboratory experiments significantly overestimate the bedload transport rate.

Keywords: Bedload, Sediment Availability, Hysteresis, Geophones, Geomorphology

1. Introduction

The bedload transport equations used in the technical literature of sediment transport are based on physical parameters such as discharge, slope and sediment size. They also implicitly assumed an infinite sediment stock. As in most watersheds, there are widespread areas of sediment production and storage, the abundance of sediment makes, at a first glance, this approximation quite realistic. This paper takes a closer look at this issue.

Located in South-West Swiss Alps, the Navisence River is hydrologically undisturbed in its upper part (down to Zinal). At the Mottec's outlet, the catchment area covers 80 km^2 , including about 50 km^2 of glaciers (Figure 1A). Its flow regime is typically glacio-nival, with very low flow rates in Winter and high discharges in July, with significant circadian variations. In Summer discharges ranging from 5 to $15 \text{ m}^3 \text{ s}^{-1}$ are measured, with peaks exceeding $30 \text{ m}^3 \text{ s}^{-1}$ during storm-induced floods. This pseudo-periodical behaviour has made it possible to study a large number of cycles with rising / falling limbs.

Bedload transport rate behaviour is influenced by anthropogenic structures. Schematically (Figure 1B), upstream of the station, there is a gravel pit, then, a transfer reach, followed by a deposition and a meandering zone. Sediment lateral inputs are currently small. Yet, some tributaries prone to debris flows such as the Péterey stream can yield large amounts of poorly sorted materials to the Navisence. In Zinal, a monitoring station has been built to measure the bedload transport rates by the means of 12 geophones mounted on steel plates fixed on the river bed (Rickennann et. al. 2012).

Bedload behaviour over time presents homogenous phases, which are analysed by using principal component analysis (PCA). We will show that its results are confirmed by field observations. To that end, i) we will specify the notions of incipient motion and average transport conditions, ii) we will present the relationships between the water and sediment fluxes, iii) we will introduce the notion of sediment availability (*i.e.* sediment on the bed which are not hidden or armoured and easily entrained by water) and then compare the empirical bedload equations.

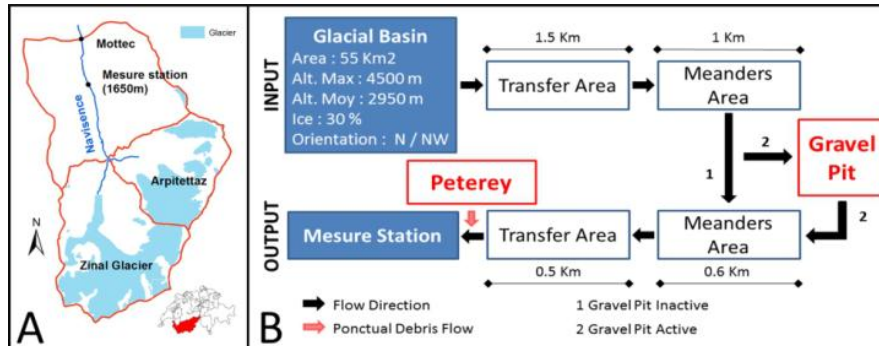


Figure 1 : A) Navisence watershed map B) Navisence behaviour scheme

2. Facilities and Methods

The gauging station consists of 12 geophones across the river bed. These geophones record the vibrations induced by the sediment when impacting the steel plates. The signal is pre-processed by transforming the vibrations into a number of pulses per minute, which will be served as a proxy for the bedload transport rate.

Part of the sediment flux (involving the finest particles) cannot be measured using this system.

These data, derived from the raw records, gather 5 events in a set of 69 days.

- The bedload transport rate is determined by summing the number of pulses per minute recorded for all of the geophones at time t . This value is then averaged for the last 24, 48 and 72 hours.
- The water discharge represents the water flux in m^3s^{-1} averaged over a timespan of one minute for the last 24, 48 and 72 hours.
- The meteorological conditions are characterized by the amount of rainfall averaged over 24 hours in mm, the maximum rainfall intensity in mm h^{-1} and the positive degree-day for the last 24h in $^{\circ}\text{C/d}$ (recorded at an altitude of 2900 m).

After centering and reducing the data, we use principal component analysis to decrease the number of dimensions. Identifying homogenous subsets of data, the result are then analysed with a hierarchical clustering that calculate distance with the Euclidian method, and classify them with the Ward method. By a trial and error process, we select the adequate number of groups.

3. Results

The dimension reduction let us select the fourth principal components that explain at least 80% of the data. Figure 3 illustrates the evolution of Q_s related to Q_w between May and August 2013. Using hierarchical classification, 6 distinct groups have been identified and projected on the time axis. Information related to special events (floods, debris flows) and about the gravel pit activity has also been added.

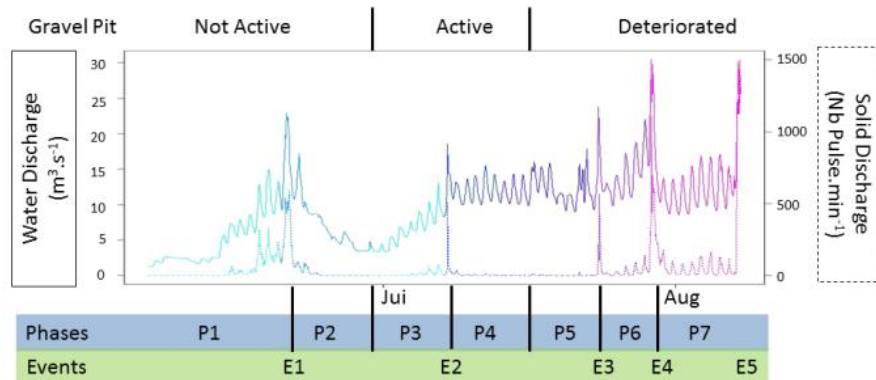


Figure 2 : Water and sediment discharges, gravel pit activities, events (E) and periods (P) identified phases for 2013

During phases P1 and P3, the system is in a transient state. Average flows and daily fluctuations increase until the first flood E1 occurs. Phase P2 corresponds to the discharge decay. Note that daily fluctuations decrease significantly. Bedload transport rates increase during P3, but suddenly drop to zero when event E2 occurs. Later on, a period of intense snow melting begins (high circadian fluctuations with a daily mean discharge above $10 \text{ m}^3 \text{ s}^{-1}$). P4 and P5 do not differ much (they are still characterized by low bedload transport rates). During P6 and P7, the water discharge is still high, and significant bedload transport occurs after the event E3. The separation by PCA highlights the role of disturbing flood events as hinges between homogenous phases.

For most phases identified by PCA the linear coefficient of determination is good ($R^2 > 0.8$), suggesting that $Q_s \sim Q_w$ can be considered homogeneous within a phase. Two subsequent distinct phases can be characterized by their parameters (Figure 4). For example, Q_d is not constant and tends to increase between P1 and P4. By contrast, T_{mean} decreases at the same time. (*e.g.* in Summer, owing to highly fluctuating water discharges, the critical water discharge is higher for particles of the same size).

For each identified period, two parameters have been defined (Figure 3):

- The critical water discharge related to incipient motion (Q_d).
- The average transport rate (T_{mean}) characterized by a linear relationship between the sediment and water discharges.

Finally, we compare these results with field observations and sediment inputs and movements upstream of the measurement station.

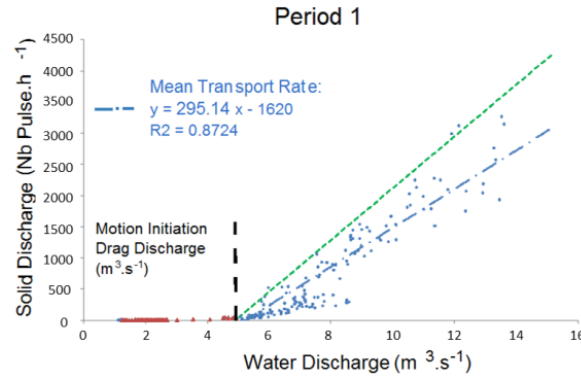


Figure 3: Relationship between the discharge (Q_d) and the water discharge (Q_w) allowing empirical estimation of the mean transport rate (T_{mean}).

For the 1 min averaged values and during each flood event, an anti-clockwise hysteresis curve has been observed, with the important consequence that the bedload transport peak is recorded after the flood peak.

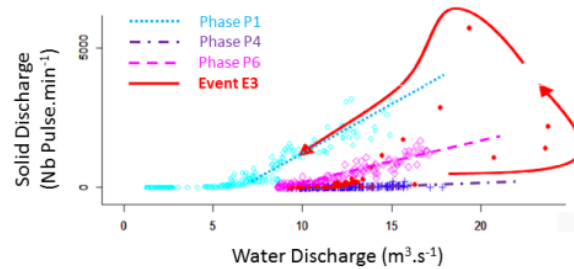


Figure 4 : $Q_s \sim Q_w$ relationship sample and flood

The important mean transport rate during phase P1 is to be linked with the stoppage of gravel-pit operations (see Fig. 1B). During E3, the entrance dyke, managing the gravel-pit has been eroded and a part of the flow stopped passing through this anthropogenic deposition area.

4. Discussion

The flood that occurred on July 1st 2012 was characterized by a water discharge, whose daily average was about $20 \text{ m}^3 \text{ s}^{-1}$. This event remobilized part of the riverbed including the deposit of a gravel bank ($D_{50} \sim 25 \text{ cm}$) just upstream of the measuring station.

During phases 1 and 2, the gravel pit was inactive and sediment transfer of sediment from upstream can be regarded as complete and undisturbed. In the first phase, sediment transport rates were observed despite the low water discharges. In the second phase, the water discharge is of the same order of magnitude, so the ratio of transport decreases significantly. We assume that the water discharge during this event allowed the sediment deposited during the falling limb of the flood of 2012 to be mobilized again and transported. The absence of pulses observed during P2 was related to the absence of sediment transport. A set of two hypotheses can validate these observations:

- **H1:** There is sediment transport in the river during this phase, but the sedimentary volume has not yet reached the station. This implies that the the bulk of the sediment volume is located far upstream.
- **H2:** There is a dependence of the critical water discharge on the sediment mobilized. In our observations we can assume that the observed water flows are able to mobilize only part of the whole grain size distribution as those deposited during the 2012 flood.

When phase P3 started, the gravel pit was “activated”, *i.e.* most of the river was diverted into the trapping area and sediment supply from upstream of the gravel dropped to a significant degree. Phases P1 and P3 are hydrologically similar. However, the mean transport rates were higher during P1, which implies that a control parameter of the system under investigation changed. Owing to the gravel-pit activation we assume that this control parameter was the sediment availability in the upper part of the system.

The event E2 marked a break between P3 and P4. During P4, T_{mean} was almost zero and Q_d was high. We assume that there is a sediment shortage during the event E2, and despite high water discharges, no sediment could be mobilized between the gravel pit and the station. The diversion dyke of the gravel pit was completely destroyed during E5 as the mean transport increased steadily from P5 to P7. We assume that material trapped in the gravel-pit was then remobilized by the Navisence and transported with some delay to the station.

In other studies, the timing of passage may cause both clockwise and counter-clockwise hysteresis (Lisle *et al.*, 2001, Parker *et al.*, 2007), but measurements in the Navisence river shows only counter-clockwise hysteresis.

4. Conclusions

Although bedload transport exhibits substantial fluctuations, statistical analysis makes it possible to determine periods during which the relationship between the sediment transport and water flow rates are closely related. For each period, we defined two parameters: the critical water discharge and the mean transport rate. T_{mean} is characterized by a high value of the coefficient of determination and thus can be considered representative of the bedload transport for the given period. The variation of these parameters over the year shows that the periods are very different from each other in term of bedload transport rate behaviour.

The field observations showed that the activities of the gravel-pit substantially affected bedload transport measurement far downstream.

Unlike the laboratory experiments of cycled hydrographs, our field measurements show that the relationship $Q_s \sim Q_w$ always form a counter-clockwise hysteresis curve. To understand this difference, we will develop in 2014 a system based on RFID system that will focus on the speed and the origin of sediments for a particular event.

5. References

- Parker, G., M. Hassan, and P. Wilcock, Adjustment of the bed surface size distribution of gravel-bed rivers in response to cycled hydrographs, *Developments in Earth Surface Processes*, 11, 241-285, 2007
- Rickenmann, D.; Turowski, J.M.; Fritschi, B.; Klaiber, A. and A. Ludwig. 2012. Bedload transport measurements at the Erlenbach stream with geophones and automated basket samplers. *Earth Surf. Process. Landf.* 37: 1000-1011
- Lisle, T.E., Cui, Y., Parker, G., Pizzuto, J.E. & Dodd, A.M., 2001. The dominance of dispersion in the evolution of bed material waves in gravel-bed rivers. *Earth Surface Processes and Landforms*, 26: 1409-1420.